

Multi-Triphenylamine-Substituted Porphyrin-Fullerene Conjugates as Charge Stabilizing “Antenna–Reaction Center” Mimics

Francis D'Souza,^{*,†} Suresh Gadde,[†] D.-M. Shafiqul Islam,[‡] Channa A. Wijesinghe,[†] Amy L. Schumacher,[†] Melvin E. Zandler,[†] Yasuyuki Araki,[‡] and Osamu Ito^{*,‡}

Department of Chemistry, Wichita State University, 1845 Fairmount, Wichita, Kansas 67260-0051, and Institute of Multidisciplinary Research for Advanced Materials, Tohoku University, Katahira, Sendai 980-8577, Japan

Received: April 23, 2007

A new concept of charge stabilization via delocalization of the π -cation radical species over the donor macrocycle substituents in a relatively simple donor–acceptor bearing multimodular conjugates is reported. The newly synthesized multimodular systems were composed of three covalently linked triphenylamine entities at the meso position of the porphyrin ring and one fulleropyrrolidine at the fourth meso position. The triphenylamine entities were expected to act as energy transferring antenna units and to enhance the electron donating ability of both free-base and zinc(II) porphyrin derivatives of these pentads. Appreciable electronic interactions between the meso-substituted triphenylamine entities and the porphyrin π -system were observed, and as a consequence, these moieties acted together as an electron-donor while the fullerene moiety acted as an electron-acceptor in the multimodular conjugates. In agreement with the spectral and electrochemical results, the computational studies performed by the DFT B3LYP/3-21G(*) method revealed delocalization of the frontier highest occupied molecular orbital (HOMO) over the triphenylamine entities in addition to the porphyrin macrocycle. Free-energy calculations suggested that the light-induced processes from the singlet excited state of porphyrins are exothermic in the investigated multimodular conjugates. The occurrence of photoinduced charge-separation and charge-recombination processes was confirmed by the combination of time-resolved fluorescence and nanosecond transient absorption spectral measurements. Charge-separated states, on the order of a few microseconds, were observed as a result of the delocalization of the π -cation radical species over the porphyrin macrocycle and the meso-substituted triphenylamine entities. The present study successfully demonstrates a novel approach of charge-stabilization in donor–acceptor multimodular conjugates.

Introduction

Over the last three decades, a great deal of research effort has been invested in the study of artificial constructs that mimic the photoinduced electron-transfer (PET) lying at the heart of photosynthetic solar energy conversion and in developing molecular electronics.^{1–12} Both covalently linked and supramolecularly assembled donor–acceptor dyads and polyads (triads, tetrads, etc.) have been elegantly designed and studied. In the construction of such dyads and polyads, porphyrins^{4,10} and fullerenes¹² have been employed as primary electron-donor and -acceptor entities, respectively, although ferrocene, carotene, or tetrathiafulvalene entities have often been utilized as terminal electron-donors.¹¹ Porphyrins as electron-donors, as well as sensitizers, are suitable for efficient electron-transfer. The rich and extensive absorption features of porphyrins guarantee an increased absorption cross-section and an efficient use of the solar spectrum.⁴ Fullerenes are excellent electron-acceptors for incorporation into artificial reaction centers.¹³ Their relatively negative reduction potentials, low solvent and internal reorganization energies, low susceptibility to solvent stabilization of the radical anion, and potential ability to act as electron

accumulators are qualities that enhance their performance.¹⁴ As a consequence, fullerenes in donor–acceptor dyads and polyads accelerate forward electron-transfer (k_{CS}) and slow down backward electron-transfer (k_{CR}), thus generating the much desired long-lived charge-separated states.¹⁴ Hence, a combination of both chromophores (i.e., porphyrins and fullerenes) seems ideal for enhancing the light-harvesting efficiency throughout the solar spectrum and for converting the harvested light into the high-energy state of the charge-separation by PET.^{15–18}

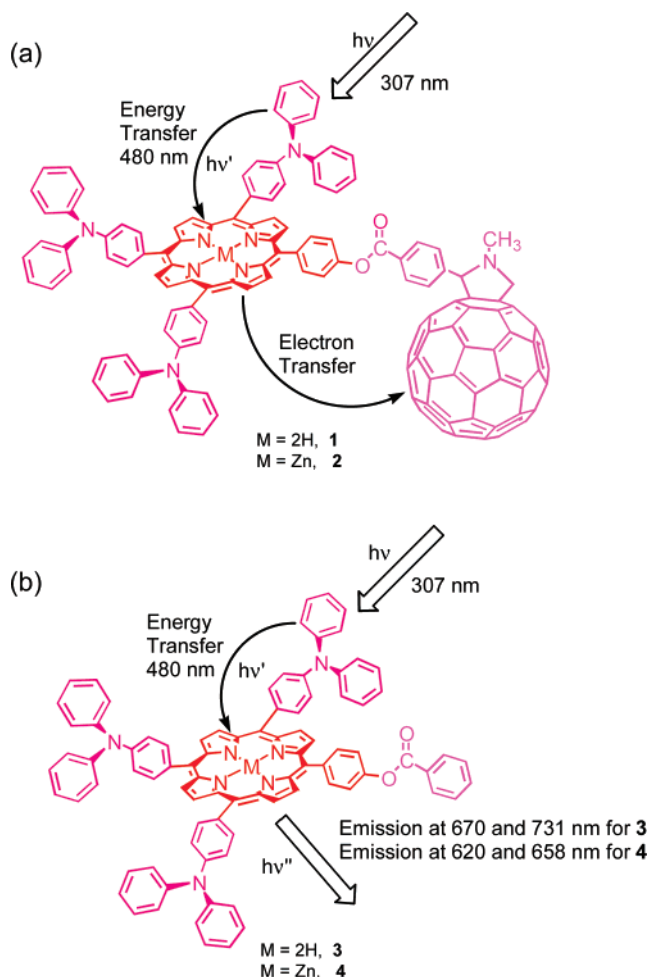
More recently, researchers have begun incorporating not only photoinduced charge-separation but also antenna functionality into artificial photosynthetic constructs.¹⁹ The structures of photosynthetic reaction centers of bacteria,³ a “nanobiological machine” of Mother Nature, and other organisms have provided important hints on the design of photosynthesis mimics. Natural antennae, including chlorophylls and carotenoids, collect large amounts of solar energy and redirect it as electronic excitation energy to the reaction center, where subsequent conversion into chemical energy takes place through redox active molecules such as chlorophylls and quinones across a photosynthetic membrane. In the developed artificial systems, energy funneling antenna molecules have been elegantly connected to the donor–acceptor systems to probe sequential energy and electron-transfer processes, thus mimicking the complex “antenna–reaction center” functionality of photosynthesis.¹⁹

* To whom correspondence should be addressed. (F.D.) E-mail: Francis.DSouza@wichita.edu; (O.I.) E-mail: ito@tagen.tohoku.ac.jp.

[†] Wichita State University.

[‡] Tohoku University.

SCHEME 1: Molecular Structure Depicting the Photochemical Events of the Multimodular Donor–Acceptor Systems Developed in the Present Study



In the present study, we report novel multimodular systems as charge stabilizing antenna–reaction center mimics. The structures of the studied molecules are comprised of three entities of triphenylamines, which absorb energy in the UV region and act as a transferring antenna in addition to the electron-donating entities, and a porphyrin moiety, which acts as an energy-acceptor from the triphenylamines and promotes electron-transfer to the fullerene entity by using the excitation energy, with the fullerene being the electron-acceptor (Scheme 1). The employed triphenylamine is a strong fluorophore, absorbing at about 300 nm and emitting in the 480 nm region.²⁰ Because of the close proximity of the triphenylamine entities to the porphyrin π -ring in the multimodular conjugates, modulation of the electronic properties of porphyrin, that is, delocalization of the porphyrin π -system to the triphenylamine entities, is expected. As demonstrated here, such delocalization will result in slowing down the undesired charge-recombination process during electron-transfer, thus generating relatively long-lived charge-separated species. Hence, the present multimodular conjugates are not only novel systems to probe sequential antenna–reaction center events but are also involved in generating relatively long-lived charge-separated states as a result of delocalization of the donor, porphyrin π -system to the antenna units. The sequential energy-transfer followed by electron-transfer results in the generation of long-lived charge-separated states, which replicates different aspects of natural photosynthesis.

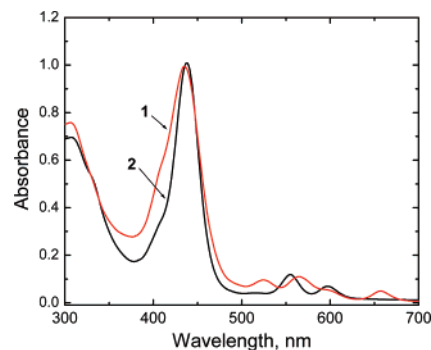


Figure 1. Optical absorption spectrum of **1** and **2** in *o*-DCB.

Results and Discussion

The structures of the newly synthesized donor–acceptor bearing multimodular systems, 5-[2-(4''-benzoic acid-4'-phenyl ester)-*N*-methyl-3,4-fulleropyrrolidine]-10,15,20-tri(*N,N*-diphenylaminophenyl) porphyrin (**1**) and 5-[2-(4''-benzoic acid-4'-phenyl ester)-*N*-methyl-3,4-fulleropyrrolidine]-10,15,20-tri(*N,N*-diphenylaminophenyl) porphyrinatozinc(II) (**2**), and their reference compounds that bear a phenyl moiety instead of the fullerene moiety, 5-(benzoic acid-4'-phenyl ester)-10,15,20-tri(*N,N*-diphenylaminophenyl) porphyrin (**3**) and 5-(benzoic acid-4'-phenyl ester)-10,15,20-tri(*N,N*-diphenylaminophenyl) porphyrinatozinc(II) (**4**) are shown in Scheme 1. We have employed both free-base and zinc porphyrins because of their different emission and redox properties.^{10a,20} The first oxidation potential of these porphyrins generally follows the trend zinc porphyrin < free-base porphyrin. As a result, it has been possible to probe the variation in the free-energy change of photoinduced electron-transfer in the studied compounds.

Absorption and Fluorescence Studies. Figure 1 shows the optical absorption spectra of conjugates **1** and **2** in *o*-dichlorobenzene (*o*-DCB). Both compounds revealed a band around 307 nm corresponding to the triphenylamine entities. The porphyrin Soret and visible bands of compounds **1**–**4** were broad and red-shifted by nearly 20 nm as compared to pristine free-base and zinc tetraphenylporphyrins (H₂TPP and ZnTPP), suggesting interactions between the porphyrin π -system and peripheral substituents. Similar results were also obtained in a polar solvent, benzonitrile (PhCN). Importantly, the absorption band of the triphenylamine entity in compounds **1**–**4** had no appreciable overlap with the porphyrin absorption in the 300–380 nm spectral region. Control experiments performed using pristine triphenylamine revealed a lack of absorption in the 400–700 nm spectral region. Hence, irradiation of compounds **1**–**4** at 307 nm is expected to selectively excite triphenylamine units, although exciting these compounds at any one of the porphyrin absorption peaks is expected to selectively excite the porphyrin macrocycle. The appended fullerene entity in **1** and **2** appeared as a shoulder at 328 nm.

When excited at the most intense visible band maxima (430–440 nm), the fluorescence spectra of **1** and control compound **3** (which has a phenyl entity instead of a fullerene entity) revealed emission bands at 670 and 732 nm, respectively. Additionally, the emission bands of **2** and control compound **4** were located at 620 and 665 nm, respectively. However, the emissions of **1** and **2** are quenched by over 90% as compared to their control compounds. As will be demonstrated later, this is due to PET from the singlet excited porphyrin to the fullerene entity. It should be mentioned here that the porphyrin emission maxima are red-shifted by 20–25 nm as compared to their tetraphenylporphyrin analogues, which is a trend similar to that observed for absorption maxima of these compounds.

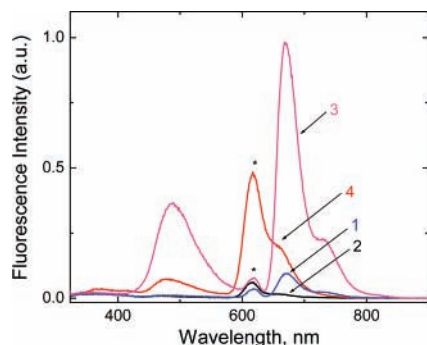


Figure 2. Fluorescence spectrum of **1**, **2**, and control compounds **3** and **4** in *o*-DCB. The concentration of porphyrins was held at 20 μ M, and the triphenylamine moieties were excited at $\lambda_{\text{max}} = 307$ nm. The asterisk indicates instrument grating line.

As shown in Figure 2, when compounds **3** and **4** were excited at 307 nm, corresponding to the absorption maxima of the peripheral triphenylamine substituents, a new emission band around 480 nm was observed. Control experiments performed using triphenylamine confirmed that this band is due to the emission of peripheral substituents. As compared with the pristine triphenylamine fluorescence, the triphenylamine emission in the case of the porphyrin derivatives was considerably quenched. For controls **3** and **4**, scanning the emission wavelength into the near-IR region also revealed additional bands corresponding to porphyrin emissions, which were not observed for the pristine porphyrins (H_2TPP and ZnTPP) with the 307 nm excitation. Excitation spectra of **3** and **4**, recorded by fixing the emission monochromator to the porphyrin emission maxima (670 and 732 nm for the zinc and free-base porphyrins, respectively), revealed spectra with the triphenylamine absorption shown in Figure 1 (also see Figure S1 Supporting Information). These results indicate that, in case of compounds **3** and **4**, the observed porphyrin emission in the near-IR region (Figure 2) is a result of singlet energy-transfer from the peripheral triphenylamine entities to porphyrin and is not a consequence of the direct excitation of porphyrin macrocycles. Interestingly, for compounds **1** and **2**, the emission corresponding to the peripheral substituents at 480 nm and the porphyrin emission in the near-IR region were almost completely quenched, which suggest the occurrence of additional photochemical events. An excited energy-transfer from the peripheral substituents to the porphyrin followed by electron-transfer from the excited porphyrin to the covalently linked fullerene entity is envisioned. In addition, a direct energy- or electron-transfer from the excited triphenylamine to the distinctly located fullerene entity must be considered to be the cause of the complete quenching of the excited triphenylamine. In the more polar benzonitrile solvent, more efficient quenching of the triphenyl and porphyrin emissions was observed.

Electrochemistry, Spectral Characterization of Porphyrin π -Cation Radicals, and Free-Energy Calculations. Furthermore, electrochemical studies using cyclic voltammetric techniques were performed to evaluate the redox potentials of the conjugates and also to evaluate the energetics of electron-transfer processes. The electrochemistry of free-base and zinc porphyrins has been extensively studied in the literature.²¹ These compounds are known to undergo two one-electron reductions, which lead to the formation of π -anion radical and dianion species, and two one-electron oxidations, which lead to the formation of π -cation radical and dication species, respectively. Figure 3 shows a cyclic voltammogram of representative conjugate **1** in *o*-DCB containing 0.1 M (*n*-Bu₄N)ClO₄, and the redox potential data are listed in Table 1. The first oxidation and the first

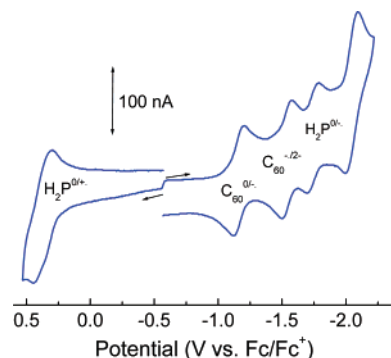


Figure 3. Cyclic voltammograms of **1** in *o*-DCB, 0.1 M (*n*-Bu₄N)ClO₄. Scan rate = 100 mV/s.

TABLE 1: Electrochemical Redox Potentials (V vs Fc/Fc⁺), Energy Levels of the Charge-Separated States (ΔG_{RIP}), and Free-Energy Changes for Charge-Separation (ΔG_{CS}) for the Multimodular Systems

compound	solvent	E_{ox} (TPA-P ^{0/+}) (V)	E_{red} (C ₆₀ ^{0/+}) (V)	$-\Delta G_{\text{RIP}}^a$ (eV)	$-\Delta G_{\text{CS}}^S$ (eV)
1	<i>o</i> -DCB	0.37	-1.16	1.41	0.54
	PhCN	0.39	-1.01	1.35	0.60
2	<i>o</i> -DCB	0.15 ^c	-1.15	1.18	0.89
	PhCN	0.18 ^c	-1.02	1.15	0.92

^a $\Delta G_{\text{RIP}} = E_{\text{ox}} - E_{\text{red}} + \Delta G_{\text{S}}$, where $\Delta G_{\text{S}} = -e^2/(4\pi\epsilon_0\epsilon_{\text{R}}R_{\text{C1-C2}})$ and ϵ_0 and ϵ_{R} refer to the vacuum permittivity and the dielectric constant of the employed solvents, respectively. ^b $-\Delta G_{\text{CS}} = \Delta E_{0-0} - \Delta G_{\text{RIP}}$, where ΔE_{0-0} is the energy of the lowest excited states (2.07 eV for ¹ZnP*, and 1.95 eV for ¹H₂P*). ^c Quasi-reversible.

reduction of all of the studied porphyrins (**1–4**) were found to be reversible, as judged from their peak-to-peak separation (ΔE_{pp}) values and from their cathodic-to-anodic peak current ratios.²² The oxidation potentials were cathodically shifted over 100 mV as compared to their tetraphenylporphyrin analogues. Scanning the potential further into the anodic direction revealed additional peaks; however, at these potentials, films started to form on the electrode surface.

The HOMO–LUMO gap for **1**, calculated from the first oxidation potential and the first fullerene spheroid centered reduction potential, was 1.53 and 1.40 V in *o*-DCB and PhCN, respectively. For **2**, these values were 1.30 and 1.20 V in *o*-DCB and PhCN, respectively. It is also important to note that the calculated HOMO–LUMO gap for **1** and **2** is smaller by about 100 mV as compared to the earlier reported tetraphenylporphyrin–fullerene derivatives in the literature,^{17,18} which is due to the effects caused by the triphenylamine entities.

Further, to aid in the interpretation of the transient spectral data discussed in the latter part of the present paper, it was essential to spectrally characterize the porphyrin π -cation radical species because of the different nature of the porphyrin macrocycle employed in the present study. Figure 4 shows the spectra of chemically oxidized porphyrins **3** and **4**. Similar spectral results were obtained during spectroelectrochemical measurements. Both free-base and zinc porphyrins exhibited distinct spectral bands in the near-IR region. The free-base porphyrin π -cation radical of compound **3** revealed bands at 500 and 750 nm, and the zinc porphyrin π -cation radical of compound **4** revealed bands at 770 and 1294 nm in *o*-DCB. It is important to note that the position of the 1294 nm band was far away from the spectral region where the triplet absorption of porphyrin and fullerene is expected to appear (500–720 nm region). Such spectrally isolated cation radical bands should help us not only in identifying the electron-transfer products but also

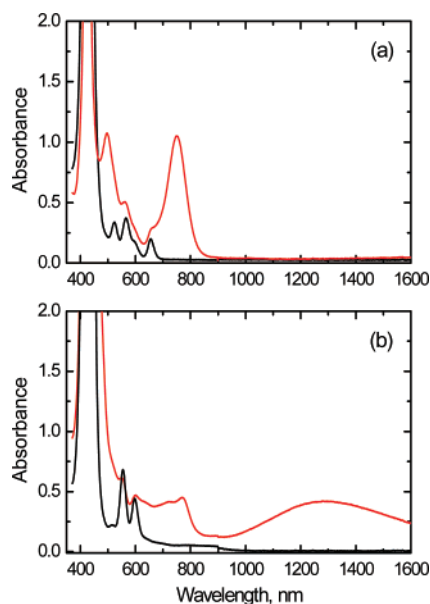


Figure 4. Visible-NIR spectra of neutral (dark line) and chemically oxidized, using equimolar nitronium hexafluoroantimonate, (red line) of (a) **3** and (b) **4** in *o*-DCB.

in following the kinetics of electron-transfer without the interference of triplet absorption bands, a problem often encountered in traditionally used tetraphenylporphyrin based donor–acceptor systems.^{17,18}

DFT B3LYP/3-21G(*) Studies. To gain insights into the geometry and the electronic structure, computational studies were performed using density functional methods (DFT) at the B3LYP/3-21G(*) level on **2**. The B3LYP/3-21G(*) methods²³ have recently been successfully used to predict the geometry and the electronic structure of molecular and supramolecular donor–acceptor assemblies.²⁴ Compound **2** was optimized to a stationary point on the Born–Oppenheimer potential energy surface whose structure is shown in Figure 5a. The center-to-center distance between the porphyrin (Zn center) and the fullerene entities was ~ 18.5 Å with no significant interactions between them. The distance between the Zn and the N atom of the triphenylamine entities was 9.2 Å, and this value was compared to the distances 18.3, 22.8, and 27.4 Å between the center of the C₆₀ to the N atoms of the triphenylamine entities. These results clearly show triphenylamine entities disposed away from the C₆₀ entity, but they are much closer to the porphyrin. In the optimized structure, the majority of the HOMO was located on the porphyrin macrocycle with considerable contribution also on the peripheral triphenylamine entities, whereas the LUMO was fully localized on the fullerene entity (Figure 5b). These results suggest the triphenylamine-substituted porphyrin is an electron-donor and fullerene is an electron-acceptor in electron-transfer reactions.²⁴ The computed gas phase HOMO–LUMO gap was 1.47 eV, which compared well with the electrochemically measured HOMO–LUMO gap in nonaqueous solvents (1.53 and 1.40 V in *o*-DCB and PhCN, respectively). The appearance of part of the HOMO over the peripheral triphenylamine substituents is expected to stabilize the radical cation by delocalization and is further slowed down in the charge-recombination process during the light-induced electron-transfer process.

The energy levels of the charge-separated states (ΔG_{RIP}) were evaluated using the Weller-type approach,²⁵ utilizing the redox potentials and the dielectric constant of the employed solvents as listed in Table 1. By comparing the energy levels of the charge-separated states with the energy levels of the excited

states, the driving forces (ΔG_{CS}) were also evaluated. The generations of $((\text{Ph}_2\text{N})_3\text{-ZnP})^{*\text{+}}\text{-C}_{60}^{*\text{-}}$ in **2** and $((\text{Ph}_2\text{N})_3\text{-H}_2\text{P})^{*\text{+}}\text{-C}_{60}^{*\text{-}}$ in **1** were exothermic via the singlet excited states of the porphyrin or the fullerene in PhCN as well as in *o*-DCB. On the basis of these calculations, an energy level diagram for **2** in PhCN is shown in Figure 6. A similar energy level diagram could also be envisioned for **1** that possesses free-base porphyrin as the primary electron-donor unit. Furthermore, the energy of the charge-separated states is lower than the porphyrin triplet state ($^3\text{H}_2\text{P}^*$ and $^3\text{ZnP}^*$), suggesting the possibility of charge-separation via the porphyrin triplet states in PhCN. However, such calculations suggested that the energy level of the charge-separated state of **1** is higher than the porphyrin triplet states in *o*-DCB, hence the electron-transfer from the triplet excited-state of the donor is endothermic for **1** in *o*-DCB, whereas charge-recombination to the triplet state is possible.

Time-Resolved Emission Studies. The time-resolved emission results tracked those of the earlier discussed steady-state emission results. Figure 7a shows the emission decay profiles of **1** and **3** in *o*-DCB and PhCN by the excitation of the porphyrin moiety. The fluorescence decay of the free-base porphyrin moiety in **3** showed mono-exponential decay (traces i and ii), with a lifetime that was close to that of the pristine free-base tetraphenylporphyrin. In the studied solvents, the fluorescence of the singlet excited porphyrin in **1** showed fast decays (traces iii and iv) that could be curve-fitted to a biexponential function involving a major short lifetime and a minor longer lifetime as listed in Table 2. As shown in Figure 7b for **4** (traces i and ii), the fluorescence time profile of the zinc porphyrin moiety also showed mono-exponential decay, with a lifetime that was close to that of the pristine zinc tetraphenylporphyrin. However, the fluorescence time profiles of **2** showed quick decays (traces iii and iv) as compared to the time profiles of reference compound **4** in both *o*-DCB and PhCN. Here also, the decay could be fitted to a biexponential fitting curve. The evaluated fluorescence lifetimes are summarized in Table 2.

These results suggest the occurrence of an excited singlet state quenching process of the porphyrins by the fullerene moiety in **1** and **2**. The quenching process of the porphyrin emission could occur from either energy-transfer or electron-transfer processes. On the basis of the observations for **2** that the time-resolved fluorescence spectra did not show the appearance of the transient fluorescence peak of the fullerene moiety after the decay of the fluorescence of the porphyrin moiety, the short lifetimes of porphyrins were predominantly ascribed to charge-separation, which was supported by the finding that the fluorescence decay rates were faster in more polar PhCN. Therefore, the rates (k_{CS}^{S}) and the quantum yields ($\Phi_{\text{CS}}^{\text{S}}$) of charge-separation were evaluated for **1** and **2** in the usual manner, and the data are shown in Table 2. The magnitudes of k_{CS}^{S} and $\Phi_{\text{CS}}^{\text{S}}$ reveal efficient charge-separation from the singlet excited-state of porphyrin moiety to fullerene in **1** and **2**.

For **2**, the k_{CS}^{S} values were $(4\text{--}5) \times 10^9 \text{ s}^{-1}$, and the $\Phi_{\text{CS}}^{\text{S}}$ values were 0.85–0.90 in *o*-DCB and PhCN, which are larger than those for **1** and suggest a relatively faster and more efficient charge-separation process in ZnP than in H₂P in polar solvents.

It should be noted that because of the delocalization of the HOMO into the peripheral triphenylamine entities in Figure 5b, the $(\text{Ph}_2\text{N})_3\text{-MP}$ moiety is expected to act as a single unit during electron-transfer from the singlet excited-state of porphyrin. Thus, these results suggest the occurrence of excited-state charge-separation in **1** and **2**, generating $((\text{Ph}_2\text{N})_3\text{-H}_2\text{P})^{*\text{+}}\text{-C}_{60}^{*\text{-}}$ and $((\text{Ph}_2\text{N})_3\text{-ZnP})^{*\text{+}}\text{-C}_{60}^{*\text{-}}$ via the excited-singlet states of

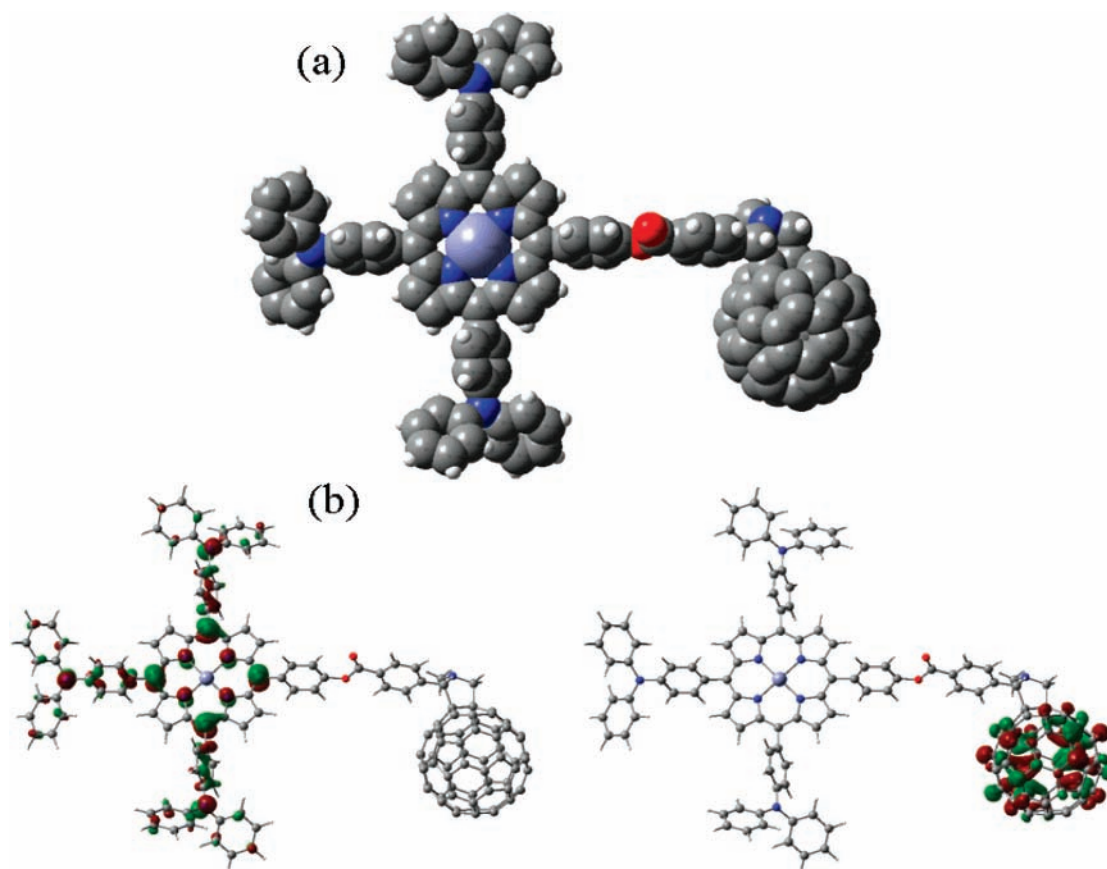


Figure 5. B3LYP/3-21G(*) optimized (a) structure and (b) the HOMO and LUMO of **2**.

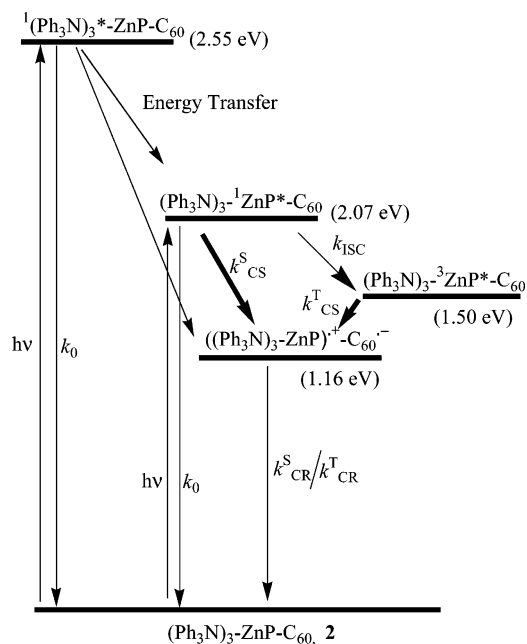


Figure 6. Energy level diagram showing different photochemical events of **2** in PhCN.

porphyrins and triphenylamine moieties. The evaluated k_{CS}^S and Φ_{CS}^S values shown in Table 2 generally follow the order **1** < **2**, that is, they depend upon the magnitude of the $-\Delta G_{CS}$ values, which suggests that this process belongs to the normal region of the Marcus parabola.

Further studies involving the nanosecond transient absorption technique were performed to identify the electron-transfer products and monitor the kinetics of charge-recombination.

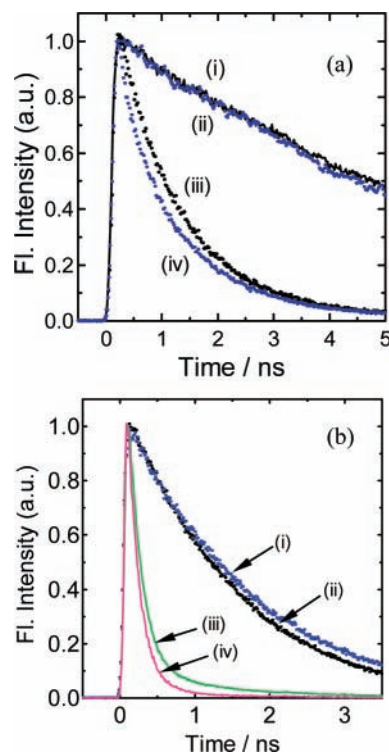


Figure 7. Fluorescence decays (a) at 660–680 nm range of (i) **3** (0.02 mM in *o*-DCB), (ii) **3** (0.02 mM in PhCN), (iii) **1** (0.02 mM in *o*-DCB), and (iv) **1** (0.02 mM in PhCN); and (b) at 600–620 nm range of (i) **4** (0.02 mM in *o*-DCB), (ii) **4** (0.02 mM in PhCN), (iii) **2** (0.02 mM in *o*-DCB), and (iv) **2** (0.02 mM in PhCN); $\lambda_{ex} = 400$ nm.

Nanosecond Transient Absorption Studies. Nanosecond transient absorption spectra of **2** observed with the 532 nm laser

TABLE 2: Fluorescence Lifetime (τ_F) of Porphyrins, Charge-Separation Rate-Constant (k_{CS}^S),^a and Charge-Separation Quantum Yield (Φ_{CS}^S) via Singlet Excited States of Porphyrins for the Multimodular Systems

compound	solvent	$\tau_F(P)$ (ns) / (fraction)	k_{CS}^S (s^{-1})	Φ_{CS}^S
1	<i>o</i> -DCB	1.11 (93%)	0.7×10^9	0.82
	PhCN	0.79 (75%)	1.1×10^9	0.87
2	<i>o</i> -DCB	0.21 (90%)	4.3×10^9	0.89
	PhCN	0.17 (95%)	5.2×10^9	0.90

^a $k_{CS}^S = ((1/\tau_{Ref}) - (1/\tau_{Conjugate}))$, $\tau_{Ref} = 6.27$ ns (in *o*-DCB) and 5.69 ns (in PhCN) for **3**, and $\tau_{Ref} = 1.85$ ns (in *o*-DCB) and 1.72 ns (in PhCN) for **4**.

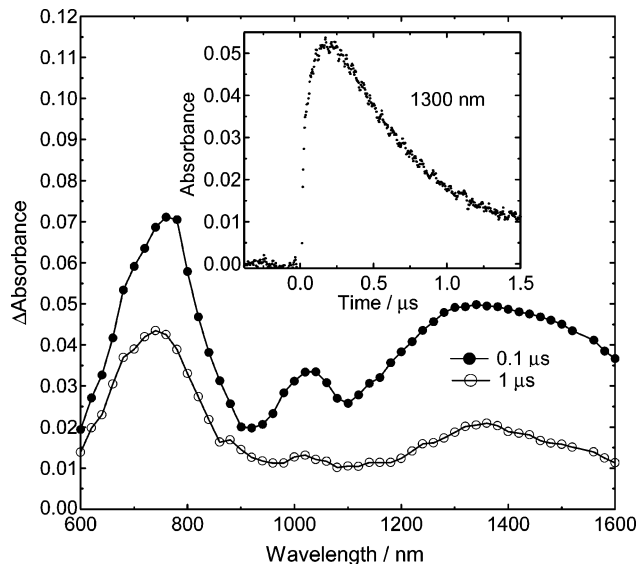


Figure 8. Nanosecond transient absorption spectra of **2** in Ar-saturated PhCN obtained by 532-nm laser light irradiation. Inset: Absorption time profile at 1300 nm.

light excitation of the ZnP moiety in deaerated PhCN are shown in Figure 8. Absorption bands appeared at 720, 840 (shoulder), 1000, and 1200–1300 nm at 100 ns after the 6 ns laser pulse excitation. Similar transient absorption spectra were also observed with 355 nm laser light excitation of **2**, where the $(Ph_2N)_3$ moiety was predominantly excited, in addition to a small fraction of the ZnP and fullerene moieties. Importantly, a peak at 1000 nm, corresponding to the formation of the fulleropyrrolidine anion radical ($C_{60}^{\bullet-}$), and an intense and broad absorption band at 1200–1300 nm, corresponding to the cation radical $[(Ph_2N)_3-ZnP]^{\bullet+}$, were observed. As mentioned earlier, the absorption peak position of $[(Ph_2N)_3-ZnP]^{\bullet+}$ was different from that typically observed for the ZnP cation radicals, where only a broad band in the 500–700 nm region was reported.^{15–18} The intense absorption band at 720 nm was also due to $[(Ph_2N)_3-ZnP]^{\bullet+}$. These results clearly demonstrate the generation of a charge-separated state $[(Ph_2N)_3-ZnP]^{\bullet+}-C_{60}^{\bullet-}$ as the main product by the excitation of either the zinc porphyrin entity or the triphenylamine entities of the multimodular system (**2**) in PhCN.

The inset of Figure 8 shows the decay time profile of $[(Ph_2N)_3-ZnP]^{\bullet+}$ at 1300 nm in PhCN; almost the same decay profile was observed for the $C_{60}^{\bullet-}$ at 1000 nm. These diagnostic peaks are useful probes for examining the reaction course of $[(Ph_2N)_3-ZnP]^{\bullet+}-C_{60}^{\bullet-}$. Both spectral time profiles exhibited the same rise and the decay, and their profiles followed a mono-exponential decay. The initial rise was slow, reaching a maximum at 200 ns, which does not correspond to the

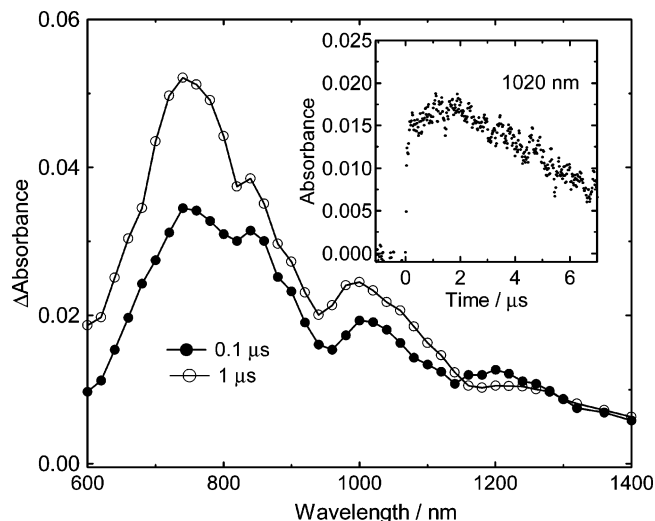


Figure 9. Nanosecond transient absorption spectra of **1** (0.08 mM) in Ar-saturated PhCN obtained by 532-nm laser light irradiation; inset: Absorption time profile at 1020 nm.

charge-separation rate evaluated from the fluorescence decay ($5.2 \times 10^9 s^{-1}$), as the half-rise should be 200 ps. Thus, the slow rise was attributed to the second charge-separation via the excited triplet species, after the fast charge-separation via the singlet excited-state of ZnP and followed by fast charge-recombination.^{14c} The rate of charge-separation (k_{CS}^T) via ${}^3ZnP^*$ was evaluated from the rise of the 1000 and 1300 nm bands for $[(Ph_2N)_3-ZnP]^{\bullet+}-C_{60}^{\bullet-}$ and was about $1.3 \times 10^7 s^{-1}$ in PhCN. The radical ion pair $(Ph_2N)_3-ZnP^{\bullet+}-C_{60}^{\bullet-}$ generated via ${}^3ZnP^*$ may have triplet spin character, which was supported by the easy quenching with added O_2 (see Supporting Information).²⁶ The rate of charge-recombination (k_{CR}^T) for $[(Ph_2N)_3-ZnP]^{\bullet+}-C_{60}^{\bullet-}$ with triplet spin character evaluated from the decay of the 1000 and 1300 nm bands was about $1.0 \times 10^6 s^{-1}$, which corresponds to the lifetime of 1000 ns in PhCN and may be far slower than the fast charge-recombination with singlet spin character.

For compound **1** in PhCN, the nanosecond transient absorption spectra recorded following 532 nm laser irradiation exhibited absorption peaks at 700, 800–840, and 1020 nm at 100 ns in PhCN (Figure 9). The transient absorption band at 1020 nm was attributed to $C_{60}^{\bullet-}$, and the cation radical of the free-base porphyrin moiety appeared around 750 nm, as was expected from Figure 4a. These spectral features support the occurrence of the excited-state charge-separation from the free-base porphyrin to the fullerene moiety, generating $[(Ph_2N)_3-H_2P]^{\bullet+}-C_{60}^{\bullet-}$. The time profile at 1020 nm showed the quick decay within the laser pulse (ca. 10 ns) that was followed by the slow rise, generating prolonged $[(Ph_2N)_3-H_2P]^{\bullet+}-C_{60}^{\bullet-}$. The quick decay may correspond to the fast charge-recombination of the radical ion pair with singlet spin character. From the slow rise, the rate for slow charge-separation via the triplet states was $k_{CS}^T = 1.0 \times 10^6 s^{-1}$ in PhCN. The rate of charge-recombination (k_{CR}^T) for $[(Ph_2N)_3-H_2P]^{\bullet+}-C_{60}^{\bullet-}$ was evaluated from the decay of the 1020 nm band and is about $5 \times 10^5 s^{-1}$, which corresponds to the 2000 ns lifetime in PhCN and is slower than k_{CR}^T for $[(Ph_2N)_3-ZnP]^{\bullet+}-C_{60}^{\bullet-}$. This suggests that they are in the inverted region of the Marcus parabola.^{2,11}

In less polar *o*-DCB with 532 nm laser excitation of **1** and **2**, quite different transient absorption spectra were observed, in which most of the bands were attributed to the triplet states (see Supporting Information), suggesting that the initial charge-

TABLE 3: Charge-Separation Rate-Constant (k_{CS}^T) via Triplet Excited State, Charge-Recombination Rate Constant (k_{CR}^T), and Lifetime of the Radical Ion-Pair (τ_{RIP}) with Triplet Spin Character for the Multimodular Conjugates in PhCN

compound	k_{CS}^T (s^{-1})	k_{CR}^T (s^{-1})	τ_{RIP} (ns)	k_{CS}^S/k_{CR}^T
1	1.1×10^6	5.0×10^5	2000	2200
2	1.3×10^7	1.0×10^6	1000	5200

recombination is faster than the 10-ns laser pulse; in addition, the second charge-separation via the triplet states is an inefficient process.

As was mentioned earlier, with the 355-nm laser pulse primarily exciting the triphenylamine moiety of **1** and **2**, energy-transfer from the excited-state of the triphenylamine moieties to the porphyrin moieties generates their excited states, from which electron-transfer takes place. In addition, direct photoejection from the triphenylamine moieties to the fullerene may occur, although this process is minor in PhCN as compared to the charge-separation process via the excited states of the porphyrin moieties.

By using the k_{CS}^S and k_{CR}^T thus evaluated in PhCN, the ratios k_{CS}^S/k_{CR}^T were evaluated as a measure of the extent of charge-stabilization in the photoinduced electron-transfer process. These values were 2200 for **1** and 5200 for **2** (Table 3). The magnitudes of k_{CR}^T , evaluated for the present multimodular systems, are smaller than the reported ones for a number of tetraphenylporphyrin–fullerene based dyads in the literature,^{14c} which is a prominent effect induced by the introduction of three triphenylamine moieties on the porphyrin core. This clearly demonstrates charge-stabilization in the present multimodular systems due to the delocalization of the radical cations as supported by the optical spectral data (Figures 1 and 3) and by the HOMO in Figure 5.

Summary

Novel multimodular systems, composed of three entities of triphenylamine, porphyrin, and fullerene, were designed, synthesized, and studied to investigate photoinduced processes by time-resolved spectroscopic methods. The spectral and computational studies revealed appreciable electronic interactions between the porphyrin π -system and the meso-substituted triphenylamine entities. The free-energy change for charge-separation and charge-recombination were evaluated and compared between $(Ph_2N)_3-ZnP-C_{60}$ and $(Ph_2N)_3-H_2P-C_{60}$. The charge-separation processes were monitored by steady-state and time-resolved emission studies, which revealed the occurrence of sequential energy-transfer and electron-transfer processes. The rate of charge-separation was found to depend on the free-energy changes. The rate of charge-recombination, as monitored by nanosecond transient absorption spectral studies, revealed charge-stabilization in these multimodular conjugates. Long-lived charge-separated states on the order of microseconds were obtained in polar PhCN, and this was attributed to the delocalization of the porphyrin π -cation radical to the triphenylamine entities. The present study offers a new route to generate long-lived charge-separated states.

Experimental Section

Chemicals. Buckminsterfullerene (C_{60} , +99.95%) was obtained from SES Research (Houston, TX). All of the reagents were from Aldrich Chemicals (Milwaukee, WI), whereas the bulk solvents utilized in the syntheses were from Fischer

Chemicals. Tetrabutylammonium perchlorate, (*n*-Bu₄N)ClO₄ used in electrochemical studies was from Fluka Chemicals.

Synthesis of Conjugates 1 and 2 and Control Compounds 3 and 4. *5-(4'-Hydroxy phenyl)-10,15,20-tri(N,N-diphenylaminophenyl) porphyrin, 1a:* In a round-bottom flask, 4 equiv of pyrrole (1.25 g, 18.5 mmol), 3 equiv of diphenyl aminobenzaldehyde (3.75 g 13.7 mmol), and 1 equiv of para hydroxybenzaldehyde (0.565 g, 4.6 mmol) were added to 250 mL of propionic acid, and the mixture was refluxed for 4 h. The solvent was removed under vacuum, and the crude product was adsorbed onto basic alumina and was purified by column chromatography on basic alumina with chloroform/methanol (91:9 v/v) as eluent. Yield ~4.6%. ¹H NMR in CDCl₃, δ (ppm) 9.0 (m, 8H, β -pyrrole-H), 8.1 (m, 6H, *ortho*-phenyl-H), 7.42 (m, 6H, *meta*-phenyl-H), 8.9, 8.1 (d, d, 4H, substituted phenyl-H), 7.0–7.16 (m, m, 30 H, N-phenyl), 5.35 (s (br), 1H, hydroxy-H), –2.79 (s, 2H, imino-H).

5-[4'-Formyl benzoic acid-4'-phenyl ester]-10,15,20-tri(N,N-diphenylaminophenyl) porphyrin, 1b: In a round-bottom flask, 100 mg of 5-(4'-hydroxyphenyl)-10,15,20-tri(N,N-diphenylaminophenyl) porphyrin (0.088 mmol), 1 equiv of 4-carboxybenzaldehyde (14 mg, 0.088 mmol), and 5 equiv of 4-di(methylamino)pyridine (DMAP, 53 mg, 0.44 mmol) were dissolved in 50 mL of dry CH₂Cl₂. The reaction mixture was cooled to 0 °C, and 5 equiv of *N,N'*-dicyclohexylcarbodiimide (DCC, 90 mg, 0.44 mmol) was slowly added. The reaction mixture was stirred for 6 h at room temperature, and the solvent was removed. The crude compound was washed with water several times and was extracted with CHCl₃. Further purification of the compound was carried out on a silica gel column using toluene and chloroform (95:5 v/v) as eluent. Yield 65%. ¹H NMR in CDCl₃, δ (ppm) 10.1 (1H, –CHO), 9.05 (m, 8H, β -pyrrole-H), 8.1 (m, 6H, *ortho*-phenyl-H), 7.47 (m, 6H, *meta*-phenyl-H), 8.9, 8.3 (d, d, 4H, substituted phenyl-H), 8.55, 7.65 (d, d, 4H, phenyl-CHO), 7.1–7.2 (m, 30 H, N-phenyl), –2.79 (s, 2H, imino-H).

5-[2-(4''-Benzoic acid-4'-phenyl ester)-N-methyl-3,4-fulleropyrrolidine]-10,15,20-tri(N,N-diphenylaminophenyl) porphyrin, 1: To 100 mL of dry toluene, compound **1b** (72 mg, 0.057 mmol), 3 equiv of C₆₀ (123 mg, 0.171 mmol), and 3 equiv of sarcosine (15 mg, 0.171 mmol) were added, and the mixture was refluxed for 12 h. Solvent was removed under vacuum, and the crude compound was adsorbed onto silica gel and was purified on a silica gel column using toluene and ethyl acetate (92:8 v/v) as eluent. Yield 37%. ESI mass in CH₂Cl₂ matrix: calculated, 2009.7; found, 2010.3. ¹H NMR in CDCl₃, δ (ppm) 8.97 (m, 8H, β -pyrrole-H), 8.1 (m, 6H, *ortho*-phenyl-H), 7.41 (m, 6H, *meta*-phenyl-H), 8.9, 8.25 (d, d, 4H, substituted phenyl-H), 8.42, 7.61 (d, d, 4H, phenyl-pyrrolidine), 7.1–7.2 (m, 30H, N-phenyl), 5.1 (s, 1H, pyrrolidine-H), 5.05, 4.31 (d, d, 2H, pyrrolidine-H) 2.84 (s, 3H, pyrrolidine N–CH₃), –2.8 (s, 2H, imino-H). UV–vis in *o*-DCB, λ (nm), 305, 333, 435.5, 525.6, 566.3, 597, 657.1.

5-[2-(4''-Benzoic acid -4'-phenyl ester)-N-methyl-3,4-fulleropyrrolidine]-10,15,20-tri(N,N-diphenylaminophenyl) porphyrinatozinc(II), 2: Pentad **1** (25 mg, 0.0124 mmol) was dissolved in 30 mL of CHCl₃, and an excess of zinc acetate (50 equiv) in methanol was added. The course of the reaction was monitored spectroscopically. At the end of the reaction (~1 h), the solvent was evaporated, and the product was purified on silica gel column using toluene as eluent. Yield 95%. ESI mass in CH₂-Cl₂ matrix: calculated, 2073.1; found, 2074.6. ¹H NMR (CS₂: CDCl₃ (1:1 v/v)) δ (ppm) 9.04 (m, 8H, β -pyrrole-H), 8.08 (m, 6H, *ortho*-phenyl-H), 7.43 (m, 6H, *meta*-phenyl-H), 9.0, 8.25

(d, d, 4H, substituted phenyl-H), 8.46, 7.61 (d, d, 4H, phenyl-pyrrolidine), 7.1–7.2 (m, 30H, N-phenyl), 5.04 (s, 1H, pyrrolidine-H), 5.0, 4.31 (d, d, 2H, pyrrolidine-H), 2.84 (s, 3H, pyrrolidine N-CH₃). UV-vis in *o*-DCB, λ (nm), 306, 330, 437.5, 554.64, 597.6.

5-[Benzoic acid-4'-phenyl ester)-10,15,20-tri(*N,N*-diphenyl-aminophenyl) porphyrin, **3**: In a round bottom flask, 100 mg of compound **1a** (0.088 mmol), 1.5 equiv of benzoyl chloride (15.3 μ L, 0.132 mmol), and 1.5 equiv of pyridine (10 μ L, 0.132 mmol) were combined in 25 mL of dry CH₂Cl₂, and the mixture was refluxed for 5 h. The solvents were removed under vacuum. The crude product was washed with water and was extracted in CHCl₃. Further purification of the compound was carried out on a silica gel column using hexanes and chloroform (9:1 v/v) as eluent. Yield 82%. ¹H NMR in CDCl₃, δ (ppm) 9.02 (m, 8H, β -pyrrole-H), 8.09 (m, 6H, *ortho*-phenyl-H), 7.47 (m, *meta*-phenyl-H), 8.92, 8.39 (d, d, 4H, substituted phenyl-H), 8.29, 7.74 (d, m, 5H, phenyl), 7.1–7.2 (m, 30H, N-phenyl), –2.79 (s, 2H, imino-H).

5-[Benzoic acid-4'-phenyl ester)-10,15,20-tri(*N,N*-diphenyl-aminophenyl) porphyrinatozinc(II), **4**: Compound **3** (50 mg, 0.0404 mmol) was added to 20 mL of CHCl₃, and an excess of zinc acetate in methanol was added. The mixture was stirred, and the course of the reaction was monitored spectroscopically. At the end of the reaction (~3 h), the solvent was evaporated, and the product was purified on a silica gel column using toluene as eluent. Yield 93%. ESI mass in a CH₂Cl₂ matrix: calculated, 1299.84; found, 1298.41. ¹H NMR CDCl₃, δ (ppm) 9.12 (m, 8H, β -pyrrole-H), 8.07 (m, 6H, *ortho*-phenyl-H), 7.47 (m, 6H, *meta*-phenyl-H), 9.02, 8.29 (d, d, 4H, substituted phenyl-H), 8.41, 7.74 (d, m, 5H, phenyl-pyrrolidine), 7.14–7.2 (m, 30H, N-phenyl), UV-vis in *o*-DCB, λ (nm), 308, 438, 556, 598.

Instrumentation. The UV-vis spectral measurements were carried out with a Shimadzu model 1600 UV-vis spectrophotometer. The steady-state fluorescence emission was monitored by a Varian Eclipse spectrometer. A right angle detection method was used. The ¹H NMR studies were carried out on Varian spectrometers at either 400 or 300 MHz. Tetramethylsilane (TMS) was used as an internal standard. Cyclic voltammograms were recorded on an EG&G model 263A potentiostat using a three electrode system in benzonitrile containing 0.1 M (*n*-Bu₄N)ClO₄ as the supporting electrolyte. A platinum button or a glassy carbon electrode was used as the working electrode. A platinum wire served as the counter electrode, and Ag/AgCl was used as the reference electrode. Ferrocene/ferrocenium (Fc/Fc⁺) redox couple was used as an internal standard. All of the solutions were purged with argon gas prior to spectral measurements.

The computational calculations were performed by the DFT B3LYP/3-21G(*) method with the GAUSSIAN-03 software package.²³ The graphics of frontier orbitals were generated using the GaussView software.

Time-Resolved Emission and Transient Absorption Measurements. The picosecond time-resolved fluorescence spectra were measured using an argon-ion pumped Ti:sapphire laser (Tsunami; pulse width = 2 ps) and a streak scope (Hamamatsu Photonics; response time = 10 ps). The details of the experimental setup are described elsewhere.²⁶ Nanosecond transient absorption measurements were carried out using the third harmonic generation (THG, 355 nm) and second harmonic generation (SHG, 532 nm) of an Nd:YAG laser (Spectra Physics, Quanta-Ray GCR-130, full-width at half-maximum (fwhm) 6 ns) as an excitation source. For the transient absorption

spectra in the near-IR region (600–1600 nm), the monitoring light from a pulsed Xe lamp was detected with a Ge-avalanche photodiode (Hamamatsu Photonics, B2834).²⁶

Acknowledgment. This work is supported by the National Science Foundation (Grant No. 0453464 to F. D.), by the donors of the Petroleum Research Fund as administered by the American Chemical Society, and by Grants-in-Aid for Scientific Research on Primary Area (417) from the Ministry of Education, Science, Sport, and Culture of Japan.

Supporting Information Available: Excitation spectrum and transient absorption spectra. This material is available free of charge via the Internet at <http://pubs.acs.org>.

References and Notes

- (1) (a) Sutin, N.; Brunschwig, B. S. *Adv. Chem. Ser.* **1990**, 226, 65. (b) Bolton, J. R.; Mataga, N.; McLendon, G.; Eds. *Adv. Chem. Ser.* **1991**, 228, 295. (c) Wheeler, R. A. *ACS Symp. Ser.* **2004**, 883, 1. (d) Leibl, W.; Mathis, P. *Electron Transfer in Photosynthesis. Series on Photoconversion of Solar Energy* **2004**, 2, 117.
- (2) (a) Marcus, R. A.; Sutin, N. *Biochim. Biophys. Acta* **1985**, 811, 265. (b) Marcus, R. A. *Angew. Chem., Int. Ed. Engl.* **1993**, 32, 1111. (c) Bixon, M.; Jortner, J. *Adv. Chem. Phys.* **1999**, 106, 35.
- (3) (a) Kirmaier, C.; Holton, D. In *The Photosynthetic Reaction Center*; Deisenhofer, J., Norris, J. R., Eds.; Academic Press: San Diego, 1993; Vol. II, pp 49–70. (b) Balzani, V.; Juris, A.; Venturi, M.; Campagna, S.; Serroni, S. *Chem. Rev.* **1996**, 96, 759.
- (4) (a) Miller, J. R.; Calcaterra, L. T.; Closs, G. L. *J. Am. Chem. Soc.* **1984**, 106, 3047. (b) Closs, G. L.; Miller, J. R. *Science* **1988**, 240, 440. (c) Connolly, J. S.; Bolton, J. R. In *Photoinduced Electron Transfer*; Fox, M. A., Chanon, M., Eds.; Elsevier: Amsterdam, 1988; Part D, pp 303–393.
- (5) (a) Wasielewski, M. R.; *Chem. Rev.* **1992**, 92, 435. (b) Kurreck, H.; Huber, M. *Angew. Chem., Int. Ed. Engl.* **1995**, 34, 849. (c) Gust, D.; Moore, T. A.; Moore, A. L. *Acc. Chem. Res.* **2001**, 34, 40.
- (6) (a) Sessler, J. S.; Wang, B.; Springs, S. L.; Brown, C. T. In *Comprehensive Supramolecular Chemistry*; Atwood J. L., Davies, J. E. D., MacNicol, D. D., Vögtle, F., Eds.; Pergamon: New York, 1996, Chapter 9. (b) Hayashi, T.; Ogoshi, H. *Chem. Soc. Rev.* **1997**, 26, 355. (c) Ward, M. W. *Chem. Soc. Rev.* **1997**, 26, 365.
- (7) (a) Balzani V.; Scandola, F. *Supramolecular Chemistry*; Ellis Horwood: New York, 1991. (b) Schlicke, B.; De Cola, L.; Belsler, P.; Balzani, V. *Coord. Chem. Rev.* **2000**, 208, 267. (c) De Silva, A. P.; Gunaratne, H. Q. N.; Gunnlaugsson, T.; Huxley, A. J. M.; McCoy, C. P.; Rademacher, J. T.; Rice, T. E. *Adv. Supramol. Chem.* **1997**, 4, 1. (d) Ashton, P. R.; Ballardini, R.; Balzani, V.; Credi, A.; Dress, K. R.; Ishow, E.; Kleverlaan, C. J.; Kocian, O.; Preece, J. A.; Spencer, N.; Stoddart, J. F.; Venturi, M.; Wenger, S. *Chem.-Eur. J.* **2000**, 6, 3558.
- (8) (a) Aviram, A.; Ratner, M., Eds. *Molecular Electronics: Science and Technology, Annals NY Acad. Sci.* **1998**, 852. (b) *Molecular Switches*; B. L. Feringa, Ed.; Wiley-VCH GmbH: Weinheim, 2001. (c) Gust D.; Moore, T. A.; Moore, A. L. *Chem. Commun.* **2006**, 1169.
- (9) (a) *Supramol. Chem.* Atwood, J. L.; Davies, J. E. D.; MacNicol, D. D.; Vögtle, F.; Reinhoudt, D. N., Eds.; Pergamon: Oxford, 1996; Vol. 10, pp 171–185. (b) Dickert, F. L.; Haunschild, A. *Adv. Mater.* **1993**, 5, 887. (c) Schierbaum, K. D.; Göpel, E. *Synth. Met.* **1993**, 61, 37. (d) de Silva, A. P.; Gunaratne, H. Q. N.; Gunnlaugsson, T.; Huxley, A. J. M.; McCoy, C. P.; Rademacher, J. T.; Rice, T. E. *Chem. Rev.* **1997**, 97, 1515. (e) Lehn, J. M. *Front. Supramol. Org. Chem. Photochem.* **1991**, 1–28. (f) Bell, T. W.; Hext, N. M. *Chem. Soc. Rev.* **2004**, 33, 589.
- (10) (a) Gust D.; Moore, T. A. In *The Porphyrin Handbook*, Kadish, K. M.; Smith, K. M.; Guillard, R., Eds.; Academic Press: Burlington, Maine, **2000**; Vol. 8, pp 153–190. (b) Imahori, H.; Sakata, Y. *Adv. Mater.* **1997**, 9, 537. (c) Prato, M. *J. Mater. Chem.* **1997**, 7, 1097. (d) Martín, N.; Sánchez, L.; Illescas, B.; Pérez, I. *Chem. Rev.* **1998**, 98, 2527. (e) Diederich, F.; Gómez-López, M. *Chem. Soc. Rev.* **1999**, 28, 263.
- (11) (a) Guldi, D. M. *Chem. Commun.* **2000**, 321. (b) Guldi, d. M.; Prato, M. *Acc. Chem. Res.* **2000**, 33, 695. (c) Guldi, D. M. *Chem. Soc. Rev.* **2002**, 31, 22. (d) Meijer, M. E.; van Klink, G. P. M.; van Koten, G. *Coord. Chem. Rev.* **2002**, 230, 141. (e) El-Khouly, M. E.; Ito, O.; Smith, P. M.; D'Souza, F. J. *Photochem. Photobiol., C.* **2004**, 5, 79. (f) Imahori, H.; Fukuzumi, S. *Adv. Funct. Mater.* **2004**, 14, 525. (g) D'Souza, F.; Ito, O. *Coord. Chem. Rev.* **2005**, 249, 1410. (h) Guldi, D. M.; Martin, N. J. *Mater. Chem.* **2002**, 12, 1978. (i) Sanchez, L.; Martin, N.; Guldi, D. M. *Angew. Chem., Int. Ed.* **2005**, 44, 5374. (j) Schuster, D. I.; Li, K.; Guldi, D. M. *C. R. Chim.* **2006**, 9, 892. (k) I. Bouamaied, T. Coskun, E. Stulz. *Struct. Bonding* **2006**, 121, 1–147.

(12) See special issue on fullerenes: *C. R. Chim.* **2006**, 9. Also, see issues 7 and 8 for review papers on this topic.

(13) (a) Allemand, P. M.; Koch, A.; Wudl, F.; Rubin, Y.; Diederich, F.; Alvarez, M. M.; Anz, S. J.; Whetten, R. L. *J. Am. Chem. Soc.* **1991**, *113*, 1050. (b) Xie, Q.; Perez-Cordero, E.; Echegoyen, L. *J. Am. Chem. Soc.* **1992**, *114*, 3978.

(14) (a) Imahori, H.; Hagiwara, K.; Akiyama, T.; Akoi, M.; Taniguchi, S.; Okada, S.; Shirakawa, M.; Sakata, Y. *Chem. Phys. Lett.* **1996**, *263*, 545. (b) Guldi, D. M.; Asmus, K. D. *J. Am. Chem. Soc.* **1997**, *119*, 5744. (c) Imahori, H.; El-Khouly, M. E.; Fujitsuka, M.; Ito, O.; Sakata, Y.; Fukuzumi, S. *J. Phys. Chem. A* **2001**, *105*, 325.

(15) (a) Imahori, H.; Yamada, K.; Hasegawa, M.; Taniguchi, S.; Okada, T.; Sakata, Y. *Angew. Chem., Int. Ed.* **1997**, *36*, 2626. (b) Luo, C.; Guldi, D. M.; Imahori, H.; Tamaki, K.; Sakata, Y. *J. Am. Chem. Soc.* **2000**, *122*, 6535. (c) Imahori, H.; Tamaki, K.; Guldi, D. M.; Luo, C.; Ito, O.; Sakata, Y.; Fukuzumi, S. *J. Am. Chem. Soc.* **2001**, *123*, 2607. (d) Imahori, H.; Araki, Y.; Sekiguchi, Y.; Ito, O.; Sakata, Y.; Fukuzumi, S. *J. Am. Chem. Soc.* **2002**, *124*, 5165. (e) Liddell, P. A.; Kodis, G.; Moore, A. L.; Moore, T. A.; Gust, D. *J. Am. Chem. Soc.* **2002**, *124*, 7668. (f) Watanabe, N.; Kihara, N.; Furusho, T.; Takata, T.; Araki, Y.; Ito, O. *Angew. Chem., Int. Ed.* **2003**, *42*, 681. (g) De la Torre, G.; Giacalone, F.; Segura, J. L.; Martin, N.; Guldi, D. M. *Chem.—Eur. J.* **2005**, *11*, 1267. (h) Georghiou, P. E.; Tran, A. H.; Mized, S.; Bancu, M.; Scott, L. T. *J. Org. Chem.* **2005**, *70*, 6158.

(16) (a) Tkachenko, N. V.; Rantala, L.; Tauber, A. Y.; Helaja, J.; Hynninen, P. H.; Lemmetyinen, H. *J. Am. Chem. Soc.* **1999**, *121*, 9378. (b) Kesti, T. J.; Tkachenko, N. V.; Vehmanen, V.; Yamada, H.; Imahori, H.; Fukuzumi, S.; Lemmetyinen, H. *J. Am. Chem. Soc.* **2002**, *124*, 8067. (c) Vehmanen, V.; Tkachenko, N. V.; Efimov, A.; Damlin, P.; Ivaska, A.; Lemmetyinen, H. *J. Phys. Chem. A* **2002**, *106*, 8029. (d) Tkachenko, N. V.; Lemmetyinen, H.; Sonoda, J.; Ohkubo, K.; Sato, K.; Imahori, H.; Fukuzumi, S. *J. Phys. Chem. A* **2003**, *107*, 8834. (e) Chukharev, V.; Tkachenko, N. V.; Efimov, A.; Guldi, D. M.; Hirsch, A.; Scheloske, M.; Lemmetyinen, H. *J. Phys. Chem. B* **2004**, *108*, 16377.

(17) (a) Imahori, H.; Hagiwara, K.; Aoki, M.; Akiyama, T.; Taniguchi, S.; Okada, T.; Shirakawa, M.; Sakata, Y. *J. Am. Chem. Soc.* **1996**, *118*, 11771. (b) Imahori, H.; Sakata, Y.; *Adv. Mater.* **1997**, *9*, 537. (c) Imahori, H.; Mori, Y.; Matano, Y. *Photochem. Photobiol., C* **2003**, *4*, 51. (d) Kuciauskas, D.; Lin, S.; Seely, G. R.; Moore, A. L.; Moore, T. A.; Gust, G.; Drovetskaya, T.; Reed, C. A.; Boyd, P. D. W. *J. Phys. Chem.* **1996**, *100*, 15926. (e) Gust, D.; Moore, T. A.; Moore, A. L. *Acc. Chem. Res.* **2001**, *34*, 40. (f) D'Souza, F.; Gadde, S.; Zandler, M. E.; Arkady, K.; El-Khouly, M. E.; Fujitsuka, M.; Ito, O. *J. Phys. Chem. A* **2002**, *106*, 12393. (g) D'Souza, F.; Deviprasad, G. R.; Zandler, M. E.; El-Khouly, M. E.; Fujitsuka, M.; Ito, O. *J. Phys. Chem. B* **2002**, *106*, 4952.

(18) (a) D'Souza, F.; Deviprasad, G. R.; El-Khouly, M. E.; Fujitsuka, M.; Ito, O. *J. Am. Chem. Soc.* **2001**, *123*, 5277. (b) D'Souza, F.; Deviprasad, G. R.; Zandler, M. E.; El-Khouly, M. E.; Fujitsuka, M.; Ito, O. *J. Phys. Chem. A* **2003**, *107*, 4801. (c) D'Souza, F.; Gadde, S.; Zandler, M. E.; Itou, M.; Araki, Y.; Ito, O. *Chem. Commun.* **2004**, 2276. (d) D'Souza, F.; Deviprasad, G. R.; Zandler, M. E.; Hoang, V. T.; Arkady, K.; VanStipdonk, M.; Perera, A.; El-Khouly, M. E.; Fujitsuka, M.; Ito, O. *J. Phys. Chem. A* **2002**, *106*, 3243. (e) El-Khouly, M. E.; Rogers, L. M.; Zandler, M. E.; Suresh, G.; Fujitsuka, M.; Ito, O.; D'Souza, F. *ChemPhysChem.* **2003**, *4*,

474. (f) D'Souza, F.; Chitta, R.; Gadde, S.; Zandler, M. E.; Sandanayaka, A. S. D.; Araki, Y.; Ito, O. *Chem. Commun.* **2005**, 1279. (g) D'Souza, F.; Smith, P. M.; Gadde, S.; McCarty, A. L.; Kullman, M. J.; Zandler, M. E.; Itou, M.; Araki, Y.; Ito, O. *J. Phys. Chem. B* **2004**, *108*, 11333. (h) D'Souza, F.; Chitta, R.; Gadde, S.; Zandler, M. E.; McCarty, A. L.; Sandanayaka, A. S. D.; Araki, Y.; Ito, O. *Chem.—Eur. J.* **2005**, *11*, 4416. (i) D'Souza, F.; Chitta, R.; Gadde, S.; McCarty, A. L.; Karr, P. A.; Zandler, M. E.; Sandanayaka, A. S. D.; Araki, Y.; Ito, O. *J. Phys. Chem. B* **2006**, *110*, 5905. (j) D'Souza, F.; Chitta, R.; Gadde, S.; Rogers, L. M.; Karr, P. A.; Zandler, M. E.; Sandanayaka, A. S. D.; Araki, Y.; Ito, O. *Chem.—Eur. J.* **2007**, *13*, 916.

(19) (a) Kodis, G.; Liddell, P. A.; de la Garza, L.; Clausen, P. C.; Lindsey, J. S.; Moore, A. L.; Moore, T. A.; Gust, D. *J. Phys. Chem. A* **2002**, *106*, 2036. (b) Kuciauskas, D.; Liddell, P. A.; Lin, S.; Johnson, T. E.; Weghorn, S. J.; Lindsey, J. S.; Moore, A. L.; Moore, T. A.; Gust, D. *J. Am. Chem. Soc.* **1999**, *121*, 8604. (c) Liddell, P. A.; Kodis, G.; de la Garza, L.; Moore, A. L.; Moore, T. A.; Gust, D. *J. Phys. Chem. B* **2004**, *108*, 10256. (d) Kodis, G.; Terazono, Y.; Liddell, P. A.; Andreasson, J.; Garg, V.; Hamburger, M.; Moore, A. L.; Moore, T. A.; Gust, D. *J. Am. Chem. Soc.* **2006**, *128*, 1818. (e) D'Souza, F.; Smith, P. M.; Zandler, M. E.; McCarty, A. L.; Itou, M.; Araki, Y.; Ito, O. *J. Am. Chem. Soc.* **2004**, *126*, 7898. (f) Wolffs, M.; Hoeben, F. J. M.; Beckers, E. H. A.; Schenning, A. P. H. J.; Meijer, E. W. *J. Am. Chem. Soc.* **2005**, *127*, 13484.

(20) Huang, C.-W.; Chiu, K. Y.; Cheng, S.-H. *Dalton Trans.* **2005**, 2417.

(21) Kadish, K. M.; Caemelbecke, E. V.; Royal, G. *Electrochemistry of Metalloporphyrins in Nonaqueous Media*, In *The Porphyrin Handbook*, Kadish, K. M.; Smith, K. M.; Guillard, R., Eds; Academic Press: San Diego, CA, 2000; Vol. 8.

(22) *Electrochemical Methods: Fundamentals and Applications* 2nd Ed. Bard, A. J.; Faulkner, L. R., Eds; John Wiley: New York, 2001.

(23) Frisch, M. J.; Trucks, G. W.; Schlegel, H. B.; Scuseria, G. E.; Robb, M. A.; Cheeseman, J. R.; Zakrzewski, V. G.; Montgomery, J. A.; Stratmann, R. E.; Burant, J. C.; Dapprich, S.; Millam, J. M.; Daniels, A. D.; Kudin, K. N.; Strain, M. C.; Farkas, O.; Tomasi, J.; Barone, V.; Cossi, M.; Cammi, R.; Mennucci, B.; Pomelli, C.; Adamo, C.; Clifford, S.; Ochterski, J.; Petersson, G. A.; Ayala, P. Y.; Cui, Q.; Morokuma, K.; Malick, D. K.; Rabuck, A. D.; Raghavachari, K.; Foresman, J. B.; Cioslowski, J.; Ortiz, J. V.; Stefanov, B. B.; Liu, G.; Liashenko, A.; Piskorz, P.; Komaromi, I.; Gomperts, R.; Martin, R. L.; Fox, D. J.; Keith, T.; Al-Laham, M. A.; Peng, C. Y.; Nanayakkara, A.; Gonzalez, C.; Challacombe, M.; Gill, P. M. W.; Johnson, B. G.; Chen, W.; Wong, M. W.; Andres, J. L.; Head-Gordon, M.; Replogle, E. S.; Pople, J. A. *Gaussian 03*; Gaussian, Inc.: Pittsburgh, Pennsylvania, 2003.

(24) For a general review on DFT applications of porphyrin—fullerene systems see Zandler, M. E.; D'Souza, F. *C. R. Chim.* **2006**, *9*, 960.

(25) (a) Rehm, D.; Weller, A. *Isr. J. Chem.* **1970**, *7*, 259. (b) Mataga, N.; Miyasaka, H. In *Electron Transfer*; Jortner, J.; Bixon, M., Eds.; John Wiley & Sons: New York, 1999; Part 2, pp 431–496.

(26) (a) Matsumoto, K.; Fujitsuka, M.; Sato, T.; Onodera, S.; Ito, O. *J. Phys. Chem. B* **2000**, *104*, 11632. (b) Komamine, S.; Fujitsuka, M.; Ito, O.; Morikawa, K.; Miyata, K.; Ohno, T. *J. Phys. Chem. A* **2000**, *104*, 11497.